

Graph Blind Deconvolution with Sparseness Constraint

Kazuma Iwata, Koki Yamada, *Student Member, IEEE*, and Yuichi Tanaka, *Senior Member, IEEE*

Abstract—We propose a blind deconvolution method for signals on graphs, with the exact sparseness constraint for the original signal. Graph blind deconvolution is an algorithm for estimating the original signal on a graph from a set of blurred and noisy measurements. Imposing a constraint on the number of nonzero elements is desirable for many different applications. This paper deals with the problem with constraints placed on the exact number of original sources, which is given by an optimization problem with an ℓ_0 norm constraint. We solve this non-convex optimization problem using the ADMM iterative solver. Numerical experiments using synthetic signals demonstrate the effectiveness of the proposed method.

Index Terms—Graph signal processing, network diffusion, non-convex optimization, sparse constraint

I. INTRODUCTION

SIGNALS diffused on a network often have very few original sources. For example, rumors on social networks and spike waves on brain networks begin spreading from very few active sources. An estimation of the source positions on the networks from observed signals, called graph signal deconvolution, is an important task in graph signal processing (GSP) [1], [2]. GSP is an extension of classical signal processing theory to signals on graphs [1]–[17]. The techniques of graph signal deconvolution are based on classical blind deconvolution algorithms for images [18], [19]. Blind deconvolution is a method for restoring an original signal from blurred measurement(s) without knowledge of the information of the spreading, that is, filters.

Extensions of blind deconvolution to the graph domain have been studied in [20], [21]. The target signal in these studies was modeled as a signal diffused by a graph filter. Graph filters are a special class of linear operators whose input and output are graph signals. Mathematically, graph filters are defined as a linear transformation that can be expressed as a polynomial of the graph variation operator [1], [2], [10]. Graph blind deconvolution simultaneously estimates the coefficients of the graph filter and the original signal. The number of original sources is expressed using the ℓ_0 constraint. However, because the ℓ_0 pseudo-norm is a non-convex function, it is generally difficult to use for optimization. In [20], the ℓ_1 -norm constraint, a convex relaxation of the ℓ_0 pseudo-norm, is used

instead of the ℓ_0 constraint. For this reason, it is not possible to strictly limit the number of signal sources in the restored signal.

In this letter, we consider a graph blind deconvolution problem that estimates an original signal having only a small number of nonzero elements from noisy signals diffused on a graph. In particular, we assume that the number of signal sources S is given a priori. We formulate a non-convex optimization problem with an S -sparse constraint and solve it using ADMM [22]. Non-convex optimization problems often converge to the local minima; however, the iterative ADMM solver works well for such a non-convex optimization with an appropriate initial value [23]. Our proposed method shares a similar proposal with graph blind deconvolution [20]; however, the previous study did not specify the number of signal sources of the original signal. Finally, we provide an illustrative experiment conducted on a synthetic dataset and compare the results with those of the conventional method. The results show that our constraint effectively estimates the signal sources, even under noisy situations.

II. PROBLEM FORMULATION

Let $\mathcal{G} = (\mathcal{V}, \mathcal{E}, \mathbf{W})$ denote an undirected graph, where \mathcal{V} and \mathcal{E} represent sets of nodes and edges, respectively. An $N \times N$ matrix \mathbf{W} contains edge weights, with $w_{ij} = w_{ji}$ denoting a positive weight of an edge connecting nodes i and j , and $w_{ij} = 0$ if there is no edge. A graph signal defined on \mathcal{V} can be represented as a vector $\mathbf{x} = [x_0, \dots, x_{N-1}]^T$, where x_i represents the signal value at node i . A graph variation operator \mathbf{S} is a matrix derived from \mathbf{W} . Its examples are graph Laplacian or adjacency matrix. Assuming that \mathbf{S} is diagonalizable, the graph variation operator can be decomposed into $\mathbf{S} = \mathbf{V}\mathbf{\Lambda}\mathbf{V}^{-1}$, where $\mathbf{\Lambda} \in \mathbb{R}^{N \times N}$ is a diagonal matrix. Based on the graph variation operator \mathbf{S} , a linear graph filter is given by

$$\mathbf{H} := \sum_{l=0}^{L-1} h_l \mathbf{S}^l, \quad (1)$$

where $\mathbf{h} = [h_0, \dots, h_{L-1}]^T$ represents the filter coefficients. Using the spectral decomposition of \mathbf{S} , the graph filter and signal can be represented in the graph frequency domain. The filtering operation is given by $\mathbf{y} = \mathbf{H}\mathbf{x}$, where \mathbf{y} is the filtered signal and \mathbf{x} is the original signal.

Graph filters and signals can be represented in the frequency domain. Let us define the matrices $\mathbf{U} = \mathbf{V}^{-1} \in \mathbb{R}^{N \times N}$ and $\mathbf{\Psi} \in \mathbb{R}^{N \times L}$, where $\Psi_{ij} = (\Lambda_{ii})^{j-1}$. Using them, the frequency representation of the signal \mathbf{x} and filter \mathbf{h} is defined as $\hat{\mathbf{x}} = \mathbf{U}\mathbf{x}$ and $\hat{\mathbf{h}} = \mathbf{\Psi}\mathbf{h}$, respectively. Therefore, given a

K. Iwata and K. Yamada are with the Graduate School of BASE, Tokyo University of Agriculture and Technology, Tokyo 184-8588, Japan (e-mail: k_iwata@msp-lab.org, k-yamada@msp-lab.org).

Y. Tanaka is with the Graduate School of BASE, Tokyo University of Agriculture and Technology, Tokyo 184-8588, Japan, and also with the PRESTO, Japan Science and Technology Agency, Kawaguchi 332-0012, Japan (e-mail: ytnk@cc.tuat.ac.jp).

This work was supported in part by JST CREST under grant JPMJCR1784 and JST PRESTO under grant JPMJPR1935.

measurement $\mathbf{y} \in \mathbb{R}^N$, we can obtain its frequency-domain representation by $\hat{\mathbf{y}} = \mathbf{U}\mathbf{y} = \text{diag}(\Psi\mathbf{h})\mathbf{U}\mathbf{x}$.

Suppose that the number of active sources in the original signal is equal to or less than S . The graph blind deconvolution is formulated as the following problem:

$$\text{find } \{\mathbf{h}, \mathbf{x}\} \text{ s.t. } \hat{\mathbf{y}} = \text{diag}(\Psi\mathbf{h})\mathbf{U}\mathbf{x}, \|\mathbf{x}\|_0 \leq S. \quad (2)$$

The first constraint in (2) can be rewritten as $\hat{\mathbf{y}} = (\Psi^T \odot \mathbf{U}^T)^T \text{vec}(\mathbf{x}\mathbf{h}^T)$, where \odot denotes the Khatri-Rao product and $\text{vec}(\cdot)$ is the vectorization operator. Let us define $\mathbf{Z} := \mathbf{x}\mathbf{h}^T$ and $\mathbf{M} := (\Psi^T \odot \mathbf{U}^T)^T$. The following problem may then be considered from (2):

$$\min_{\mathbf{Z}} \text{rank}(\mathbf{Z}) \text{ s.t. } \hat{\mathbf{y}} = \mathbf{M}\text{vec}(\mathbf{Z}), \|\mathbf{Z}\|_{2,0} \leq S, \quad (3)$$

where $\|\mathbf{Z}\|_{2,0}$ is equal to the number of nonzero rows of \mathbf{Z} . The rank and $\ell_{2,0}$ pseudo-norm minimization are generally combinatorial and NP-hard. In [20], to make (3) tractable, the nuclear norm $\|\mathbf{Z}\|_*$ is utilized as a convex relaxation of the rank function. Similarly, the $\ell_{2,1}$ mixed norm $\|\mathbf{Z}\|_{2,1}$ is the closest convex relaxation of $\|\mathbf{Z}\|_{2,0}$ [24]. As a result, in the existing method [20], problem (3) is transformed into the following convex optimization problem:

$$\min_{\mathbf{Z}} \|\mathbf{Z}\|_* + \tau \|\mathbf{Z}\|_{2,1} \text{ s.t. } \hat{\mathbf{y}} = \mathbf{M}\text{vec}(\mathbf{Z}). \quad (4)$$

The accuracy of the estimation can be improved by using multiple measurements. We consider P measurements $\{\mathbf{y}_p\}_{p=1}^P$, where each different sparse input is diffused by the common filter \mathbf{H} . Multiple signals are then treated as a vector of stacked measurements $\hat{\mathbf{y}} = [\hat{\mathbf{y}}_1^T, \dots, \hat{\mathbf{y}}_P^T]^T \in \mathbb{R}^{NP}$, and similarly for the unobserved inputs $\tilde{\mathbf{x}} = [\mathbf{x}_1^T, \dots, \mathbf{x}_P^T]^T \in \mathbb{R}^{NP}$. In addition, the matrices are $\mathbf{Z}_p = \mathbf{x}_p\mathbf{h}^T, p = 1, \dots, P$, and let the vertical and horizontal matrices be $\tilde{\mathbf{Z}}_v = [\mathbf{Z}_1^T, \dots, \mathbf{Z}_P^T]^T \in \mathbb{R}^{NP \times L}$ and $\tilde{\mathbf{Z}}_h = [\mathbf{Z}_1, \dots, \mathbf{Z}_P] \in \mathbb{R}^{N \times PL}$, respectively. The formulation using multiple measurements is then given as follows:

$$\min_{\{\mathbf{Z}_p\}_{p=1}^P} \|\tilde{\mathbf{Z}}_v\|_* + \tau \|\tilde{\mathbf{Z}}_h\|_{2,1} \text{ s.t. } \tilde{\mathbf{y}} = (\mathbf{I}_P \otimes \mathbf{M})\text{vec}(\tilde{\mathbf{Z}}_h). \quad (5)$$

III. S-SPARSE CONSTRAINT

A. Formulation of Sparseness Constraint

For simplicity, we consider the single-input case in (4). However, the method introduced in this section can be easily extended to the multiple-input case in (5).

In fact, problem (4) cannot strictly limit the number of signal sources, although it is a convex optimization problem. Instead, we consider the following problem to constrain the exact sparseness of \mathbf{Z} .

$$\min_{\mathbf{Z}} \text{rank}(\mathbf{Z}) \text{ s.t. } \|\hat{\mathbf{y}} - \mathbf{M}\text{vec}(\mathbf{Z})\|_2 < \epsilon, \|\mathbf{Z}\|_{2,0} \leq S, \quad (6)$$

where $\epsilon > 0$. Here, let us define the indicator function of the inequality constraint on the $\ell_{2,0}$ mixed pseudo-norm in (6) as

$$\mathcal{I}_{\|\cdot\|_{2,0} \leq S}(\mathbf{X}) = \begin{cases} 0 & \text{if } \|\mathbf{X}\|_{2,0} \leq S, \\ \infty & \text{otherwise.} \end{cases} \quad (7)$$

The graph blind deconvolution with the S -sparse constraint in (6) can then be reformulated as follows:

$$\min_{\mathbf{Z}} \|\mathbf{Z}\|_* + \mathcal{I}_{\|\cdot\|_{2,0} \leq S}(\mathbf{Z}) \text{ s.t. } \|\hat{\mathbf{y}} - \mathbf{M}\text{vec}(\mathbf{Z})\|_2 < \epsilon, \quad (8)$$

where we use the relaxation of the rank function as in (4). Further, we modify (8) by introducing local variables $\mathbf{Z}_1, \mathbf{Z}_2 \in \mathbb{R}^{N \times L}$ such that the problem can be applied to an iterative solver based on the ADMM:

$$\begin{aligned} \min_{\mathbf{Z}} \|\mathbf{Z}_1\|_* + \mathcal{I}_{\|\cdot\|_{2,0} \leq S}(\mathbf{Z}_2) + \mathcal{I}_{\mathcal{D}}(\mathbf{W}) \\ \text{s.t. } \mathbf{Z}_i = \mathbf{W}, i = 1, 2, \end{aligned} \quad (9)$$

where $\mathcal{I}_{\mathcal{D}}(\cdot)$ is an indicator function for $\mathcal{D} = \{\mathbf{Z} \in \mathbb{R}^{N \times L} \mid \|\hat{\mathbf{y}} - \mathbf{M}\text{vec}(\mathbf{Z})\|_2 < \epsilon\}$. The constraint in (9) ensures that all local variables are identical to \mathbf{W} . We solve (9) with the following iterations:

$$\begin{aligned} \mathbf{W}^{(n+1)} = \arg \min_{\mathbf{W}} \mathcal{I}_{\mathcal{D}}(\mathbf{W}) \\ + \rho \|\mathbf{W} - \frac{1}{2} \sum_{k=1}^2 (\mathbf{Z}_k^{(n)} - \mathbf{Y}_k^{(n)})\|_F, \end{aligned} \quad (10)$$

$$\mathbf{Z}_1^{(n+1)} = \arg \min_{\mathbf{Z}} \|\mathbf{Z}\|_* + \frac{\rho}{2} \|\mathbf{Z} - (\mathbf{W}^{(n+1)} + \mathbf{Y}_1^{(n)})\|_F, \quad (11)$$

$$\begin{aligned} \mathbf{Z}_2^{(n+1)} = \arg \min_{\mathbf{Z}} \mathcal{I}_{\|\cdot\|_{2,0} \leq S}(\mathbf{Z}) \\ + \frac{\rho}{2} \|\mathbf{Z} - (\mathbf{W}^{(n+1)} + \mathbf{Y}_2^{(n)})\|_F, \end{aligned} \quad (12)$$

$$\mathbf{Y}_k^{(n+1)} = \mathbf{Y}_k^{(n)} + \mathbf{W}^{(n+1)} - \mathbf{Z}_k^{(n+1)} \quad k = 1, 2. \quad (13)$$

The indicator function in (12) is non-convex because a set satisfying the S -sparse constraint is a non-convex set. Therefore, the optimization problem becomes non-convex. Although ADMM is a method for solving a class of convex optimization problems, it has been validated as effective for non-convex optimization problems in practice [22], [25].

B. Optimization with S -sparse Constraint

The following is equivalent to (12):

$$\text{find } \mathbf{Z}^* \in \arg \min_{\mathbf{Z} \in \{\mathbf{Z} \mid \|\mathbf{Z}\|_{2,0} \leq S\}} \|\mathbf{Z} - \bar{\mathbf{Z}}\|_F, \quad (14)$$

where $\bar{\mathbf{Z}} = \mathbf{W}^{(n+1)} + \mathbf{Y}_2^{(n)}$. This is the projection onto a set satisfying the S -sparse constraint. In other words, minimization can be performed by calculating the projection onto the $\ell_{2,0}$ mixed pseudo-norm ball. Projection (14) might appear to be difficult; however, its optimal solution can be computed in a closed form, which is given by the following result:

Proposition 1. Let $\bar{\mathbf{Z}} = [\bar{\mathbf{z}}_1, \dots, \bar{\mathbf{z}}_N]^T$, i.e., $\bar{\mathbf{z}}_1, \dots, \bar{\mathbf{z}}_N$ are the rows of $\bar{\mathbf{Z}}$ in (14). In addition, let $\bar{\mathbf{z}}_{(1)}, \dots, \bar{\mathbf{z}}_{(N)}$ be the vectors $\bar{\mathbf{z}}_1, \dots, \bar{\mathbf{z}}_N$ sorted in descending order in terms of their ℓ_2 norms, that is, $\|\bar{\mathbf{z}}_{(1)}\|_2 \geq \|\bar{\mathbf{z}}_{(2)}\|_2 \geq \dots \geq \|\bar{\mathbf{z}}_{(N)}\|_2$. The index $\cdot_{(k)}$ corresponds to the index of the k -th largest row in terms of their norm. The projection (14) can be written as follows:

$$\text{find } \mathbf{Z}^* \in \arg \min_{\mathbf{Z} \in \mathbb{R}^{N \times L}} \|\mathbf{Z} - \bar{\mathbf{Z}}\|_F^2 \text{ s.t. } \|\mathbf{Z}\|_{2,0} \leq S. \quad (15)$$

One minima of (15) is given by

$$\mathbf{Z}^* = \begin{cases} \bar{\mathbf{Z}} & \text{if } \|\bar{\mathbf{Z}}\|_{2,0} \leq S, \\ \left[\tilde{\mathbf{z}}_1^T, \dots, \tilde{\mathbf{z}}_N^T \right]^T & \text{if } \|\bar{\mathbf{Z}}\|_{2,0} > S, \end{cases} \quad (16)$$

where

$$\tilde{\mathbf{z}}_i = \begin{cases} \bar{\mathbf{z}}_{(i)} & \text{if } i \in \{1, \dots, S\}, \\ \mathbf{0} & \text{if } i \in \{S+1, \dots, N\}. \end{cases} \quad (17)$$

Thus, the projection onto the $\ell_{2,0}$ mixed pseudo-norm ball is equivalent to preserving the top S rows of $\bar{\mathbf{Z}}$ according to their ℓ_2 norms.

Proof. Because the case of $\|\bar{\mathbf{Z}}\|_{2,0} \leq S$ is trivial, we consider the case of $\|\bar{\mathbf{Z}}\|_{2,0} > S$. To satisfy the inequality constraint $\|\mathbf{Z}\|_{2,0} \leq S$ in (15), at least $N - S$ subvectors of \mathbf{Z}^* must be zero vectors from the definition of $\ell_{2,0}$ mixed pseudo-norm. Meanwhile, any change in \mathbf{Z}^* from $\bar{\mathbf{Z}}$ increases the value of $\|\mathbf{Z} - \bar{\mathbf{Z}}\|_F^2$. From these facts, the k -th subvector of \mathbf{Z}^* of the optimal solution must consist of $\bar{\mathbf{z}}_k$ or $\mathbf{0}$. Therefore, the cost function is expressed as

$$\|\mathbf{Z} - \bar{\mathbf{Z}}\|_F^2 = \sum_{k=1}^N \|\mathbf{z}_k - \bar{\mathbf{z}}_k\|_2^2. \quad (18)$$

If we set $\mathbf{z}_k = \mathbf{0}$, the cost is increased by $\|\bar{\mathbf{z}}_k\|_2^2$. Hence, from the fact that $\|\bar{\mathbf{z}}_{(1)}\|_2 \geq \|\bar{\mathbf{z}}_{(2)}\|_2 \geq \dots \geq \|\bar{\mathbf{z}}_{(N)}\|_2$, we can conclude that setting $\mathbf{z}_{(1)} = \bar{\mathbf{z}}_{(1)}, \dots, \mathbf{z}_{(S)} = \bar{\mathbf{z}}_{(S)}$ and $\mathbf{z}_{(S+1)} = \mathbf{0}, \dots, \mathbf{z}_{(N)} = \mathbf{0}$ minimizes the cost function (18) subject to the inequality constraint $\|\mathbf{Z}\|_{2,0} \leq S$. \square

Finally, the detailed steps of our algorithm are summarized in Algorithm 1. In the algorithm, a scalar η is set to gradually decrease the value of γ , which stabilizes the ADMM for non-convex optimization, which is shown in the convergence analysis of the ADMM in the non-convex case [26], where the iterations generated by the ADMM under appropriate conditions converge to a stationary point with a sufficiently small γ . In addition, the solution of the non-convex optimization problem strongly depends on the initial value. Among the computable solutions, the closest to the optimal solution of the non-convex optimization problem is the solution of the convex relaxed optimization problem. Therefore, we recommend using the solution of the convex relaxed problem (4) as the initial value.

IV. EXPERIMENTAL RESULTS

A. Graph filter based diffusion

We validate the performance of the blind deconvolution with the S -sparse constraint by solving (8) and comparing the result with the recovery result of (4). We use an undirected random sensor graph with $N = 64$ and a community graph with $N = 100$ [27]. The graph variation operator used is the adjacency matrix of \mathcal{G} , that is, $\mathbf{S} = \mathbf{A}$. Let \mathbf{x}_0 be the original signal and $\hat{\mathbf{x}}$ be the restored signal. The root-mean-square error $\text{RMSE} = \|\hat{\mathbf{x}} - \mathbf{x}_0\|$ is used as an objective measure of the restoration performance.

Synthetic signals are modeled by $\mathbf{y} = \mathbf{H}\mathbf{x} + \epsilon$, where ϵ is an additive white Gaussian noise and the filter coefficients

Algorithm 1: Graph Blind Deconvolution with Sparseness Constraint based on ADMM

Input : $\{\hat{\mathbf{y}}_p\}_{p=1}^P, S, \mathbf{Y}_k^{(0)}$,
 $\mathbf{Z}_k^{(0)}$: Arbitrary initial value,
 $\rho > 0$, and $0 < \eta < 1$

Output: $\mathbf{W}^{(n)}$

- 1 **while** a stopping criterion is not satisfied **do**
- 2 $\mathbf{W}^{(n+1)} = \text{prox}_{\mathcal{I}_D(\cdot)} \left(\frac{1}{2} \sum_{k=1}^2 \left(\mathbf{Z}_k^{(n)} - \mathbf{Y}_k^{(n)} \right) \right)$
- 3 $\mathbf{Z}_1^{(n+1)} = \text{prox}_{\rho \|\cdot\|_*} \left(\mathbf{W}^{(n+1)} + \mathbf{Y}_1^{(n+1)} \right)$
- 4 Set $\bar{\mathbf{Z}} = \mathbf{W}^{(n+1)} + \mathbf{Y}_2^{(n+1)} = [\bar{\mathbf{z}}_1^T, \dots, \bar{\mathbf{z}}_N^T]^T$
- 5 . Compute indices $(1), \dots, (N)$ by sorting $\bar{\mathbf{z}}_1, \dots, \bar{\mathbf{z}}_N$ in descending order in terms of their ℓ_2 norms
- 6 . Set $\mathbf{z}_{(1)}^* = \bar{\mathbf{z}}_{(1)}, \dots, \mathbf{z}_{(S)}^* = \bar{\mathbf{z}}_{(S)}$ and $\mathbf{z}_{(S+1)}^* = \mathbf{0}, \dots, \mathbf{z}_{(N)}^* = \mathbf{0}$
- 7 . $\mathbf{Z}_2^{(n+1)} = [\mathbf{z}_1^{*T}, \dots, \mathbf{z}_N^{*T}]^T$
- 8 **for** $k = 1, 2$ **do**
- 9 $\mathbf{Y}_k^{(n+1)} = \mathbf{Y}_k^{(n)} + \mathbf{W}^{(n+1)} - \mathbf{Z}_k^{(n+1)}$
- 10 $\rho \leftarrow \eta \rho$
- 11 $n \leftarrow n + 1$

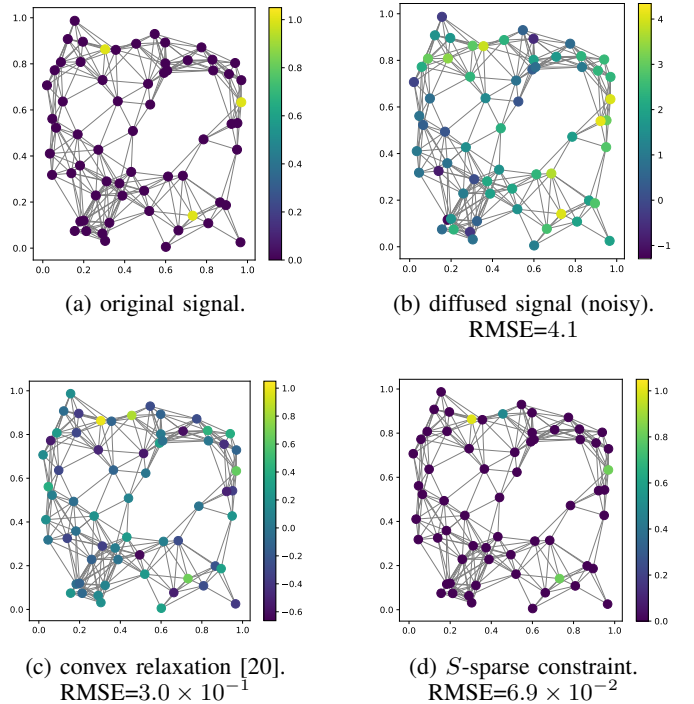


Fig. 1: Recovery results on a sensor graph with $N = 64$ and $L = 3$.

with $L = 3$ are set to $\mathbf{h} = [1.0, 0.8, 0.3]$. The number of nonzero elements in the original signal is $S = 3$. Figs. 1(a) and 2(a) show the signal sources and Figs. 1(b) and 2(b) are examples of the diffused noisy measurements. We generated 30 synthetic signals with random source locations to conduct the restoration experiment.

In all recovery experiments, we used an optimal solution

TABLE I: Average RMSE of restored signals in Experiment IV-A

Graph	Diffused signal	Convex relaxation	Proposed
Sensor	3.8	3.5×10^{-1}	5.8×10^{-2}
Community	1.5×10^1	4.3×10^{-1}	1.4×10^{-2}

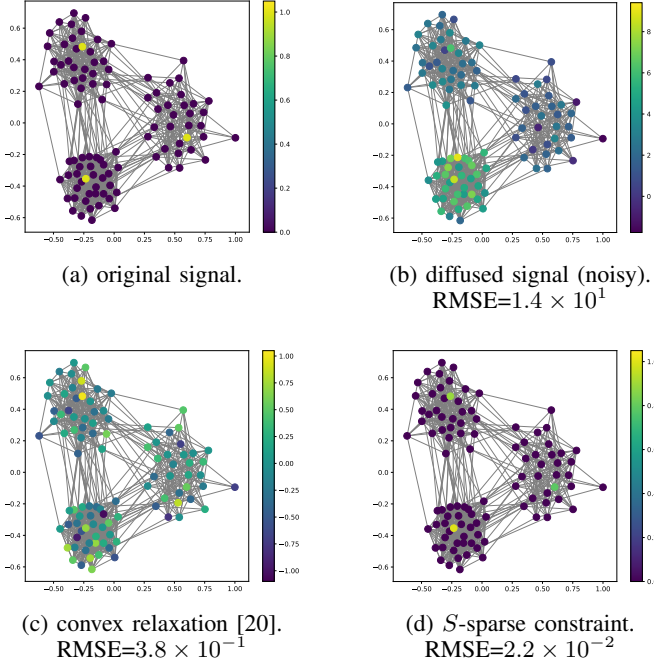


Fig. 2: Recovery results on a community graph with $N = 100$ and $L = 5$ (mismatched case).

of (4) as the initial value $Z_k^{(0)}$ of the minimization problem in (10)–(13). The RMSE values for the restoration results are shown in Table I.

Fig. 1(c) shows the result restored by the convex relaxation (4). The restored signal values have high magnitudes at the sources of the original signal; however, a few samples other than the original sources also have a high magnitude. Therefore, it is difficult to accurately estimate the position of the signal source from the restored signal. Fig. 1(d) shows the restored signal by our S -sparse constraint. It can be seen that the position of the signal source of the restored signal is clearly the same as those of the original signal.

B. Estimating the case of a mismatched graph filter order

In many cases, the order of the graph filter is not known a priori when restoring real data. Therefore, in this experiment, we set the order of the graph filter (1) to 5, which is larger than the actual filter order $L = 3$.

The RMSEs for the results are summarized in Table II. As in the previous experiment, the proposed method outperformed the existing method. Fig. 2(c) and Fig. 2(d) show the results of the convex relaxation (4) and our S -sparse constraint, respectively. Because the order of the estimated filter is different from that of the actual diffusion filter, high magnitude values appear in many places other than the original signal source in

TABLE II: Average RMSE of restored signals in Experiment IV-B

Graph	Diffused signal	Convex relaxation	Proposed
Sensor	3.8	3.9×10^{-1}	2.1×10^{-1}
Community	1.5×10^1	4.5×10^{-1}	3.1×10^{-2}

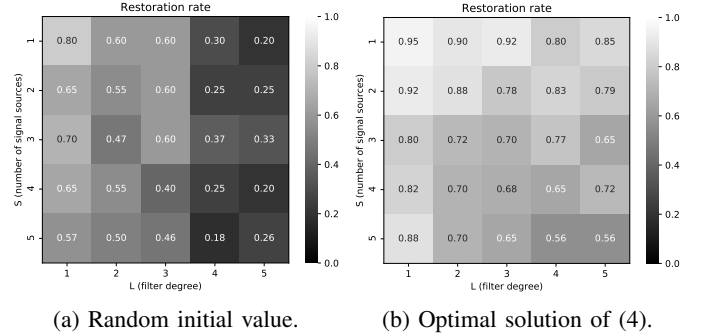


Fig. 3: Recovery performance matrix according to S and L .

Fig. 2(c). By contrast, only the signal sources can be accurately estimated by constraining the number of signal sources shown in Fig. 2(d).

C. Recovery performance for different initial values

Finally, we compared the performances between a recovery using random initial values and a recovery using the optimal solutions of the convex relaxed problem (4). In this experiment, the location of the signal source are determined at random. The filter coefficients of the graph filter are also set at random within the range of $[0, 1]$. The restoration performance is evaluated based on the ratio of the restored signal to the original signal, as given by the following:

$$r_{\text{restore}} = \frac{1}{N} \sum_{k=1}^N \frac{S_{k,\text{match}}}{S_k}, \quad (19)$$

where N is the number of trials and S and $S_{k,\text{match}}$ represent the number of original sources and the number of matched sources, respectively. Fig. 3 shows the recovery performance for each combination of the number of original sources and the order of the graph filter for signals on the random sensor graph. Because random initial values tend to fall into the local minima, the recovery performance is low even when the number of original sources is small or the order of the filter is low. When the optimal solution of the convex problem is set to the initial value, it is observed that the recovery performance is considerably improved.

V. CONCLUSION

We propose a method for identifying the original graph signal from diffused noisy measurements with the exact sparseness constraint. Our ADMM-based algorithm can recover the original signal based on a non-convex optimization problem with the ℓ_0 constraint. Numerical results demonstrate the superiority of the proposed approach over existing methods. Furthermore, we showed that appropriately setting the initial values improves the restoration performance.

REFERENCES

- [1] D. I. Shuman, S. K. Narang, P. Frossard, A. Ortega, and P. Vandergheynst, "The emerging field of signal processing on graphs: Extending high-dimensional data analysis to networks and other irregular domains," *IEEE Signal Processing Magazine*, vol. 30, no. 3, pp. 83–98, May 2013.
- [2] A. Ortega, P. Frossard, J. Kovačević, J. M. F. Moura, and P. Vandergheynst, "Graph signal processing: Overview, challenges, and applications," *Proc. IEEE*, vol. 106, no. 5, pp. 808–828, May 2018.
- [3] G. Cheung, E. Magli, Y. Tanaka, and M. Ng, "Graph spectral image processing," *Proc. IEEE*, vol. 106, no. 5, pp. 907–930, May 2018.
- [4] Y. Tanaka, Y. C. Eldar, A. Ortega, and G. Cheung, "Sampling signals on graphs: From theory to applications," *IEEE Signal Processing Magazine*, accepted, 2020.
- [5] D. K. Hammond, P. Vandergheynst, and R. Gribonval, "Wavelets on graphs via spectral graph theory," *Applied and Computational Harmonic Analysis*, vol. 30, no. 2, pp. 129 – 150, 2011. [Online]. Available: <http://www.sciencedirect.com/science/article/pii/S1063520310000552>
- [6] A. Sakiyama and Y. Tanaka, "Oversampled graph Laplacian matrix for graph filter banks," *IEEE Trans. Signal Process.*, vol. 62, no. 24, pp. 6425–6437, Dec. 2014.
- [7] A. Sakiyama, K. Watanabe, Y. Tanaka, and A. Ortega, "Two-channel critically-sampled graph filter banks with spectral domain sampling," *IEEE Trans. Signal Process.*, vol. 67, no. 6, pp. 1447–1460, Mar. 2019.
- [8] A. Sakiyama, Y. Tanaka, T. Tanaka, and A. Ortega, "Eigendecomposition-free sampling set selection for graph signals," *IEEE Trans. Signal Process.*, vol. 67, no. 10, pp. 2679–2692, May 2019.
- [9] A. Sandryhaila and J. M. F. Moura, "Discrete signal processing on graphs," *IEEE Transactions on Signal Processing*, vol. 61, no. 7, pp. 1644–1656, 2013.
- [10] —, "Discrete signal processing on graphs: Frequency analysis," *IEEE Transactions on Signal Processing*, vol. 62, no. 12, pp. 3042–3054, 2014.
- [11] S. Segarra, A. G. Marques, and A. Ribeiro, "Optimal graph-filter design and applications to distributed linear network operators," *IEEE Transactions on Signal Processing*, vol. 65, no. 15, pp. 4117–4131, 2017.
- [12] S. K. Narang and A. Ortega, "Perfect reconstruction two-channel wavelet filter banks for graph structured data," *IEEE Trans. Signal Process.*, vol. 60, no. 6, pp. 2786–2799, Jun. 2012. [Online]. Available: http://biron.usc.edu/wiki/index.php/Graph_Filterbanks
- [13] —, "Compact support biorthogonal wavelet filterbanks for arbitrary undirected graphs," *IEEE Trans. Signal Process.*, vol. 61, no. 19, pp. 4673–4685, Oct. 2013. [Online]. Available: http://biron.usc.edu/wiki/index.php/Graph_Filterbanks
- [14] M. Onuki, S. Ono, M. Yamagishi, and Y. Tanaka, "Graph signal denoising via trilateral filter on graph spectral domain," *IEEE Trans. Signal Inf. Process. Netw.*, vol. 2, no. 2, pp. 137–148, Jun. 2016.
- [15] A. Anis, A. Gadde, and A. Ortega, "Efficient sampling set selection for bandlimited graph signals using graph spectral proxies," *IEEE Trans. Signal Process.*, vol. 64, no. 14, pp. 3775–3789, Jul. 2016.
- [16] Y. Tanaka, "Spectral domain sampling of graph signals," *IEEE Trans. Signal Process.*, vol. 66, no. 14, pp. 3752–3767, Jul. 2018.
- [17] Y. Tanaka and Y. C. Eldar, "Generalized sampling on graphs with subspace and smoothness priors," *IEEE Transactions on Signal Processing*, vol. 68, pp. 2272–2286, 2020.
- [18] D. Kundur and D. Hatzinakos, "Blind image deconvolution," *IEEE Signal Processing Magazine*, vol. 13, no. 3, pp. 43–64, 1996.
- [19] A. Ahmed, B. Recht, and J. Romberg, "Blind deconvolution using convex programming," *IEEE Transactions on Information Theory*, vol. 60, no. 3, pp. 1711–1732, 2014.
- [20] S. Segarra, G. Mateos, A. G. Marques, and A. Ribeiro, "Blind identification of graph filters," *IEEE Transactions on Signal Processing*, vol. 65, no. 5, pp. 1146–1159, March 2017.
- [21] D. Ramírez, A. G. Marques, and S. Segarra, "Graph-signal reconstruction and blind deconvolution for diffused sparse inputs," in *2017 IEEE International Conference on Acoustics, Speech and Signal Processing (ICASSP)*, 2017, pp. 4104–4108.
- [22] S. Ono, " l_0 gradient projection," *IEEE Transactions on Image Processing*, vol. 26, no. 4, pp. 1554–1564, April 2017.
- [23] S. Boyd, N. Parikh, E. Chu, B. Peleato, and J. Eckstein, "Distributed optimization and statistical learning via the alternating direction method of multipliers," *Foundations and Trends in Machine Learning*, vol. 3, no. 1, pp. 1–122, 2011. [Online]. Available: <http://dx.doi.org/10.1561/2200000016>
- [24] J. A. Tropp, "Just relax: convex programming methods for identifying sparse signals in noise," *IEEE Transactions on Information Theory*, vol. 52, no. 3, pp. 1030–1051, 2006.
- [25] M. W. Berry, M. Browne, A. N. Langville, V. P. Pauca, and R. J. Plemmons, "Algorithms and applications for approximate nonnegative matrix factorization," *Computational Statistics & Data Analysis*, vol. 52, no. 1, pp. 155 – 173, 2007. [Online]. Available: <http://www.sciencedirect.com/science/article/pii/S01679473060004191>
- [26] M. Hong, Z. Luo, and M. Razaviyayn, "Convergence analysis of alternating direction method of multipliers for a family of nonconvex problems," *SIAM Journal on Optimization*, vol. 26, no. 1, pp. 337–364, 2016. [Online]. Available: <https://doi.org/10.1137/140990309>
- [27] N. Perraudin, J. Paratte, D. Shuman, L. Martin, V. Kalofolias, P. Vandergheynst, and D. K. Hammond, "Gspbox: A toolbox for signal processing on graphs," 2014.